

# Dioxygen Reactivity and Heme Redox Potential of Truncated Human Cystathionine $\beta$ -Synthase<sup>†</sup>

Sebastián Carballal,<sup>\*,§,||</sup> Peter Madzela,<sup>⊥</sup> Carlos F. Zinola,<sup>||</sup> Martín Graña,<sup>#</sup> Rafael Radi,<sup>§,||</sup> Ruma Banerjee,<sup>\*,⊥,▽</sup> and Beatriz Alvarez<sup>\*,§,||</sup>

*Laboratorio de Enzimología and Laboratorio de Electroquímica Fundamental, Facultad de Ciencias, Departamento de Bioquímica and Center for Free Radical and Biomedical Research, Facultad de Medicina, Universidad de la República, Montevideo, Uruguay, Unité de Biochimie Structurale, Institut Pasteur, 75015 Paris, France, Redox Biology Center and the Biochemistry Department, University of Nebraska, Lincoln, Nebraska 68588-0664, and Department of Biological Chemistry, University of Michigan, Ann Arbor, Michigan 48109-0606*

Received May 12, 2007; Revised Manuscript Received January 9, 2008

**ABSTRACT:** Cystathionine  $\beta$ -synthase (CBS) catalyzes the condensation of serine and homocysteine to cystathionine, which represents the committing step in the transsulfuration pathway. CBS is unique in being a pyridoxal phosphate-dependent enzyme that has a heme cofactor. The activity of CBS under in vitro conditions is responsive to the redox state of the heme, which is distant from the active site and has been postulated to play a regulatory role. The heme in CBS is unusual; it is six-coordinate, low spin, and contains cysteine and histidine as axial ligands. In this study, we have assessed the redox behavior of a human CBS dimeric variant lacking the C-terminal regulatory domain. Potentiometric redox titrations showed a reversible response with a reduction potential of  $-291 \pm 5$  mV versus the normal hydrogen electrode, at pH 7.2. Stopped-flow kinetic determinations demonstrated that Fe(II)CBS reacted with dioxygen yielding Fe(III)CBS without detectable formation of an intermediate species. A linear dependence of the apparent rate constant of Fe(II)CBS decay on dioxygen concentration was observed and yielded a second-order rate constant of  $(1.11 \pm 0.07) \times 10^5 \text{ M}^{-1} \text{ s}^{-1}$  at pH 7.4 and 25 °C for the direct reaction of Fe(II)CBS with dioxygen. A similar reactivity was observed for full-length CBS. Heme oxidation led to superoxide radical generation, which was detected by the superoxide dismutase (SOD)-inhibitable oxidation of epinephrine. Our results show that CBS may represent a previously unrecognized source of cytosolic superoxide radical.

Cystathionine  $\beta$ -synthase (CBS<sup>1</sup>, EC 4.2.1.22) is a key enzyme of homocysteine metabolism in mammals. It cata-

lyzes the condensation of homocysteine and serine to form cystathionine in the first step of the transsulfuration pathway that leads to cysteine. Mutations in CBS are the single most common cause of severe hyperhomocysteinemia (1). Increased levels of homocysteine in plasma constitute an independent risk factor for cardiovascular diseases and neural tube defects (2, 3).

CBS is present in the cytosolic compartment of several cell types and has also recently been detected in the nucleus (4). Full-length human CBS has a subunit molecular weight of ~63 kDa and exists as a homotetramer or higher order oligomers. Each polypeptide chain has a modular organization that comprises an N-terminal region that binds heme, followed by a catalytic domain that binds pyridoxal 5'-phosphate (PLP) and a C-terminal regulatory domain that binds the allosteric activator, S-adenosyl-L-methionine (AdoMet) (5, 6). CBS also has a disulfide oxidoreductase motif that contains the sequence CPGC (7, 8). Limited proteolysis results in the separation of the C-terminal AdoMet regulatory domain leading to a more active enzyme and a change in its oligomeric state to a dimer of 45 kDa subunits (5). This truncated form of the enzyme is observed in liver cells challenged with the proinflammatory cytokine, TNF $\alpha$  (9).

<sup>†</sup> This work was supported by grants from CSIC, Universidad de la República, and Programa de Desarrollo Tecnológico-II, Ministry of Education and Culture, Uruguay (to B.A.), the Howard Hughes Medical Institute and International Centre of Genetic Engineering and Biotechnology (to R.R.), and the National Institutes of Health (HL58984, to R.B.). R.R. is a Howard Hughes International Research Scholar.

<sup>§</sup> Laboratorio de Enzimología, Facultad de Ciencias, Universidad de la República.

<sup>||</sup> Laboratorio de Electroquímica Fundamental, Facultad de Ciencias, Universidad de la República.

<sup>#</sup> Departamento de Bioquímica, Facultad de Medicina, Universidad de la República.

<sup>⊥</sup> Center for Free Radical and Biomedical Research, Facultad de Medicina, Universidad de la República.

<sup>⊥</sup> University of Nebraska.

<sup>▽</sup> Institut Pasteur, Paris. Present address: Unidad de Bioinformática, Institut Pasteur, Montevideo, Uruguay.

<sup>▽</sup> University of Michigan.

\* To whom correspondence should be addressed. (B.A.) Phone/Fax: +598-2-5250749. E-mail: Beatriz.Alvarez@fcien.edu.uy. (R.B.) Phone: +1-734-615-5238. E-mail: rbanerje@umich.edu.

<sup>1</sup> Abbreviations: CBS, cystathionine  $\beta$ -synthase; Fe(III)CBS, CBS with ferric heme; Fe(II)CBS, CBS with ferrous heme; PLP, pyridoxal 5'-phosphate; AdoMet, S-adenosyl-L-methionine; NHE, normal hydrogen electrode; NBT, 4-nitroblue tetrazolium; O<sub>2</sub><sup>•-</sup>, superoxide radical; SOD, superoxide dismutase; DTPA, diethylenetriaminepentaacetic acid; K<sub>3</sub>Fe(CN)<sub>6</sub>, potassium ferricyanide; EDTA, ethylenediaminetetraacetic acid; epinephrine, 1-(3,4-dihydroxyphenyl)-2-(methylamino)ethanol; adrenochrome, 2,3-dihydro-3-hydroxy-1-methylindole-5,6-quinone.

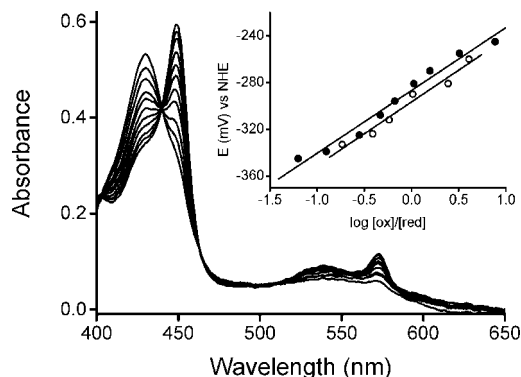


FIGURE 1: Potentiometric titration of CBS. Fe(III)CBS (7  $\mu$ M) in 50 mM sodium phosphate buffer, pH 7.2, was titrated potentiometrically with dithionite as reductant as described under Methods. Inset: Fit to the Nernst equation (eq 1) of the reductive titration with dithionite (closed circles) and the oxidative titration with ferricyanide (open circles).

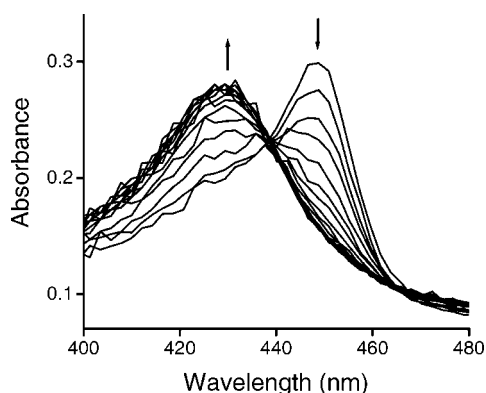


FIGURE 2: Oxidation of Fe(II)CBS by dioxygen. UV-vis absorption spectra after mixing Fe(II)CBS (5  $\mu$ M) with  $O_2$  (129  $\mu$ M) in phosphate buffer (0.1 M, pH 7.4, with 0.1 mM DTPA) at 25 °C. Spectra were collected every 8 ms after mixing, from 4 to 140 ms. The arrows indicate the direction of the absorbance change over time.

CBS is the only known PLP-dependent enzyme that also contains heme (10). The heme in CBS is an unusual iron protoporphyrin IX with an axial cysteinate ligand (Cys52), as also seen in cytochrome P450, chloroperoxidase, and nitric oxide synthase. In addition, CBS heme has as its sixth ligand a histidine residue ( $N_{\epsilon 2}$  of His65) (7). Few examples of naturally occurring Cys/His liganded proteins exist: SoxAX of bacterial thiosulfate oxidation (11), a cytochrome bound to the photosynthetic reaction center from *R. sulfidophilum* (12), the nuclear receptor E75 from *Drosophila* (13), and the heme-regulated inhibitor HRI (14). Ferric CBS exhibits a heme Soret peak at 428 nm, which shifts to 449 nm in the ferrous state (15). In both the oxidized and reduced states, the heme is six-coordinate and low spin. The function of the heme in CBS remains unknown. A catalytic role in the PLP-mediated enzymatic mechanism was initially excluded by spectroscopic studies and is consistent with its absence from the highly homologous yeast enzyme, which catalyzes the same reaction (16, 17). This was confirmed by the crystal structure, which reveals that the heme and PLP are  $\sim 20$  Å apart (7, 8). Several point mutations in the heme binding site have been identified in patients with hereditary hyperhomocysteinemia, revealing that changes in the heme environment modulate enzyme activity and/or stability (18–21).

A redox sensor role has been proposed for the heme in CBS since its reduction is correlated with a 50% decrease in the enzyme activity (15). A physiological rationale for this is the role of the transsulfuration pathway in provision of cysteine, the limiting reagent in the synthesis of glutathione. Thus, under oxidizing conditions, when glutathione pools are diminished, increasing CBS activity would increase the flux of homocysteine to cysteine and could help reestablish glutathione levels. In addition, perturbation of the heme ligand environment by mercuric chloride (22) or by reduction at elevated temperatures (23), which results in loss of the native cysteine ligand, leads to inhibition of CBS activity. Furthermore, nitric oxide (NO) and carbon monoxide (CO) bind to ferrous CBS and inhibit enzyme activity (24–26). Thus, the properties of the heme are consistent with a regulatory role that can modulate enzyme activity via redox changes or alteration in the coordination environment (26).

Understanding the redox properties of the heme in CBS is critical for evaluating its role in the cellular milieu. In this study, we determined the reduction potential of the heme in the truncated form of human CBS and investigated the reactivity of the reduced enzyme with dioxygen. Our results show that the unusual heme in CBS represents a heretofore unrecognized potential source of cytosolic superoxide radical ( $O_2^{\bullet -}$ ).

## EXPERIMENTAL PROCEDURES

**Reagents.** Catalase was purchased from Fluka and xanthine oxidase was from Calbiochem. Bovine Cu,Zn-superoxide dismutase (SOD) was obtained from DDI Pharmaceuticals (Mountain View, CA).

**Enzyme Purification.** The truncated human CBS lacking 143 amino acids at the C-terminus was purified from a recombinant expression system (pGEX4T1/hCBS $\Delta$ C143) that produces a fusion protein with glutathione *S*-transferase (27). The recombinant protein was expressed and purified, removing the glutathione *S*-transferase tag, as described previously (15). Full-length CBS was similarly obtained (15).

**Biochemical Analysis.** CBS activity was measured using the ninhydrin assay (28). The enzyme had a specific activity of  $\sim 550 \mu\text{mol h}^{-1} \text{mg}^{-1}$  at 37 °C, which is similar to reported values (5). Protein concentration was determined by the Bradford method using bovine serum albumin as standard (29). Heme content was determined by the pyridine heme-chrome assay (30). Truncated CBS had 80% heme saturation and extinction coefficients at 428 nm and pH 7.4 of  $73\,500 \pm 3700 \text{ M}^{-1} \text{cm}^{-1}$  (based on protein) and  $92\,700 \pm 4600 \text{ M}^{-1} \text{cm}^{-1}$  (based on heme). The ratio of the absorbances at 280 and 428 nm was 1.07. Thiols were quantified spectrophotometrically using 5,5'-dithiobis-(2-nitrobenzoic acid) ( $\epsilon_{412} = 13\,600 \text{ M}^{-1} \text{cm}^{-1}$ ) (31), after ultrafiltration with Ultrafree 0.5 centrifugal filter devices (Millipore) to remove interference from the cofactors at 412 nm. One free thiol per CBS monomer was measured, consistent with the reported value (32).

**Enzyme Reduction.** Reduction of Fe(III)CBS was performed under a nitrogen atmosphere by the addition of known aliquots of sodium dithionite ( $\text{Na}_2\text{S}_2\text{O}_4$ ) and confirmed by the appearance of the 449 nm peak in the UV-visible absorption spectrum. Dithionite stock solutions were prepared

in degassed 0.1 N NaOH and quantified by ferricyanide reduction ( $\epsilon_{420} = 1020 \text{ M}^{-1} \text{ cm}^{-1}$ ) (33) assuming a 2:1 stoichiometry, in agreement with the actual reductant being the dithionite dissociation product  $\text{SO}_2^{\bullet-}$  (34).

**Potentiometric Titrations.** The reduction midpoint potential ( $E_m$ ) of the heme in truncated human CBS ( $7 \mu\text{M}$  in 50 mM sodium phosphate buffer, pH 7.2) was determined potentiometrically according to the method of Dutton using sodium dithionite as reductant and potassium ferricyanide as oxidant (35). The redox mediators anthraquinone 2-sulfonate ( $E_m = -225 \text{ mV}$ ), benzyl viologen ( $E_m = -358 \text{ mV}$ ), and methyl viologen ( $E_m = -440 \text{ mV}$ ) (36) were added to the sample at  $10 \mu\text{M}$  concentrations. Redox titrations were performed at room temperature in an anaerobic chamber with 95:5 nitrogen/hydrogen and  $<1 \text{ ppm}$  dioxygen. All solutions were prepared anaerobically, and the enzyme was purged with pure nitrogen before use. The potential of the sample was measured using a FLUKE 75 III multimeter coupled to a gold working electrode and a saturated Ag/AgCl reference electrode, which was routinely calibrated. The potential values are reported versus the normal hydrogen electrode (NHE). After equilibration following each addition of reductant or oxidant, during which the measured potential drift was  $<1 \text{ mV}$  in 5 min, UV-visible absorption spectra were recorded using a diode array spectrophotometer inside the anaerobic chamber. The control spectra of the redox mediators in the absence of the enzyme were obtained in the presence of dithionite at the desired potentials. These spectra were used for subtraction from the enzyme and redox mediator samples obtained at the corresponding potentials. To obtain the  $E_m$  value, the measured potential was fit to the Nernst equation (eq 1), where the concentration of the reduced species was obtained by the difference in absorbance at 428 or 449 nm between the spectrum at a given potential and the spectrum of the fully oxidized form (in the reductive direction).

$$E = E_m + \frac{0.059}{n} \log \frac{[\text{ox}]}{[\text{red}]} \quad (1)$$

**Kinetic Studies.** The kinetics of the reaction between Fe(II)CBS and dioxygen were studied in a stopped-flow spectrophotometer (Applied Photophysics, SF17MV). Time-dependent spectra were obtained with a photodiode array accessory. Argon-purged CBS solutions in phosphate buffer (0.2 M, pH 7.4, with 0.2 mM DTPA) were fully reduced by adding anaerobic dithionite (40–100  $\mu\text{M}$ ) and transferred under a continuous flow of argon into the stopped-flow syringe. Reduced CBS was then mixed with equal volumes of solutions of increasing dioxygen concentrations obtained from mixing known volumes of anaerobic, air-equilibrated (0.258 mM  $\text{O}_2$ ), and dioxygen-equilibrated (1.25 mM  $\text{O}_2$ ) water at  $25^\circ\text{C}$  (37). Apparent rate constants for CBS oxidation were determined by fitting the absorbance decay at 449 nm resulting from CBS oxidation in the presence of SOD (0.25  $\mu\text{M}$  monomer) to a single exponential function with the software provided with the instrument. All kinetic experiments were performed at  $25^\circ\text{C}$ .

**Simulations.** Computer-assisted kinetic simulations of the oxidation of Fe(II)CBS were performed with the software Gepasi (38).

**Determination of Superoxide Radical Production by Fe(II)CBS Exposed to Dioxygen.** Superoxide radical genera-

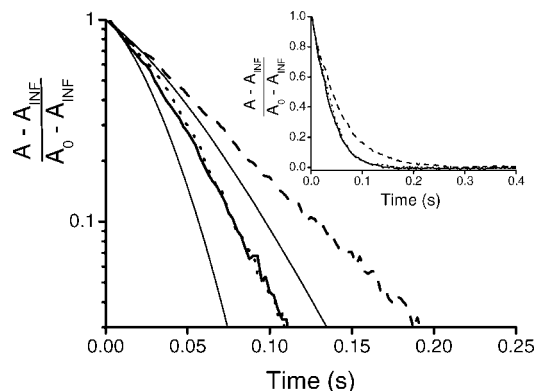


FIGURE 3: Kinetic traces of Fe(II)CBS reaction with dioxygen. Logarithmic plot of the stopped-flow traces at 449 nm after mixing Fe(II)CBS ( $4.4 \mu\text{M}$ , obtained by reduction with  $23 \mu\text{M}$  dithionite, final concentrations) with  $\text{O}_2$  (129  $\mu\text{M}$ ) in phosphate buffer (0.1 M, pH 7.4, with 0.1 mM DTPA) at  $25^\circ\text{C}$ , alone (solid line) and in the presence of SOD (0.4  $\mu\text{M}$ , dashed line), or catalase (0.2  $\mu\text{M}$ , dotted line).  $A$  is the absorbance at time  $t$ , and  $A_0$  and  $A_{\text{INF}}$  are the initial and final values, respectively. The fine lines represent the kinetic traces simulated for the reactions shown in Table 1, assuming a rate constant of  $2 \times 10^6 \text{ M}^{-1} \text{ s}^{-1}$  (upper fine line) or  $1 \times 10^7 \text{ M}^{-1} \text{ s}^{-1}$  (lower fine line) for the oxidation of Fe(II)CBS with superoxide radical ( $\text{O}_2^{\bullet-}$ ). Inset: Linear plot of the same data up to 0.4 s.

tion was determined by the SOD-inhibitable oxidation of epinephrine to adrenochrome (39, 40), which is monitored by the appearance of a characteristic peak at 480 nm ( $\epsilon_{480} = 4020 \text{ M}^{-1} \text{ cm}^{-1}$ ) (41). A typical mixture contained anaerobic CBS (25  $\mu\text{M}$ ) in Tris buffer (0.1 M, pH 8.6, with 0.2 mM EDTA) to which an equivalent amount of sodium dithionite (12.5  $\mu\text{M}$ ) was added. After CBS was fully reduced, epinephrine and dioxygen were added simultaneously to final concentrations of 2 mM and 200  $\mu\text{M}$ , respectively, in the absence or in the presence of SOD (1.5  $\mu\text{M}$  monomer). Since CBS has been reported to slowly reoxidize spontaneously in an acid-promoted process (42), these assays were carried out at a slightly alkaline pH. Epinephrine bitartrate stock solutions (40 mM) were freshly prepared daily in 0.01 N HCl, kept on ice, and added to the buffered reaction mixture immediately before use to prevent autooxidation. Oxidation products of epinephrine were determined from the UV-visible spectra after ultrafiltration to remove interference from the enzyme. Control experiments in which CBS was omitted were performed. To determine the stoichiometry of epinephrine oxidation by superoxide radical under these conditions, the reaction was compared with the reduction of ferricytochrome  $c$  at 550 nm ( $\epsilon_{550} = 21\,000 \text{ M}^{-1} \text{ cm}^{-1}$ ) (43) using xanthine/xanthine oxidase as the superoxide radical generation system.

## RESULTS

**Potentiometric Titrations.** Figure 1 shows the spectral data obtained in a representative redox titration of truncated CBS. For the reductive titration, the linear fit of the data obtained at 449 or 428 nm to the Nernst equation yielded midpoint reduction potentials of  $-287 \text{ mV}$  (slope =  $54 \text{ mV}$ ) at 449 nm and  $-285 \text{ mV}$  (slope =  $59 \text{ mV}$ ) at 428 nm, versus NHE at pH 7.2. The reduction potentials obtained from the oxidative titration were in close agreement to those derived from the reductive titration, with values of  $-293 \text{ mV}$  (slope =  $58 \text{ mV}$ ) and  $-294 \text{ mV}$  (slope =  $50 \text{ mV}$ ) at 449 and 428

Table 1: Reactions Involved in the Aerobic Oxidation of Dithionite-Reduced CBS

reaction	rate constant	reference
$\text{Fe(II)CBS} + \text{O}_2 \rightarrow \text{Fe(III)CBS} + \text{O}_2^{\cdot-}$	$1.11 \times 10^5 \text{ M}^{-1} \text{ s}^{-1}$ (pH 7.4, 25 °C)	this study
$\text{Fe(II)CBS} + \text{O}_2^{\cdot-} + 2\text{H}^+ \rightarrow \text{Fe(III)CBS} + \text{H}_2\text{O}_2$	$2\text{--}10 \times 10^6 \text{ M}^{-1} \text{ s}^{-1}$ (pH 7.4, 25 °C)	this study
$\text{S}_2\text{O}_4^{2-} \rightleftharpoons 2\text{SO}_2^{\cdot-}$	$2.5 \text{ s}^{-1}$ (f), $1.8 \times 10^9 \text{ M}^{-1} \text{ s}^{-1}$ (r) <sup>a</sup> (pH 6.5, 25 °C)	65, 66
$\text{SO}_2^{\cdot-} + \text{O}_2 \rightarrow \text{SO}_2 + \text{O}_2^{\cdot-}$	$1 \times 10^8 \text{ M}^{-1} \text{ s}^{-1}$ (pH 6.5, 25 °C)	66
$2\text{O}_2^{\cdot-} + 2 \text{H}^+ \rightarrow \text{O}_2 + \text{H}_2\text{O}_2$	$2 \times 10^5 \text{ M}^{-1} \text{ s}^{-1}$ (pH 7.4)	67

<sup>a</sup> (f), forward; (r), reverse.

nm, respectively. Thus, the redox reaction of the heme in CBS followed Nernstian behavior for a one-electron system and achieved a reversible equilibrium with the absence of any side reaction. The average  $\pm$  standard deviation for independent determinations was  $-291 \pm 5 \text{ mV}$  ( $n = 4$ ) for the dithionite titrations and  $-289 \pm 6 \text{ mV}$  ( $n = 3$ ) for the ferricyanide titrations.

**Kinetics of Fe(II)CBS Reaction with Dioxygen.** Since solutions of reduced CBS oxidize immediately upon exposure to dioxygen, the reaction of Fe(II)CBS with dioxygen had to be studied by stopped flow spectrophotometry. As shown in Figure 2, when an anaerobic solution of dithionite-reduced CBS was mixed with excess dioxygen under pseudo-first-order conditions, the reduced enzyme with the characteristic absorption peak at 449 nm converted to the oxidized state with a maximum at 428 nm, in less than 0.2 s. A clear isosbestic point was observed at 438 nm, excluding the formation of intermediates such as  $\text{Fe}^{\text{II}}/\text{O}_2$  and/or  $\text{Fe}^{\text{III}}/\text{O}_2^{\cdot-}$  at detectable levels.

The kinetic traces showed deviations from the expected single exponential function, and the logarithmic plots were not linear (Figure 3). The presence of catalase (0.2 or 1.25  $\mu\text{M}$ ) did not alter the kinetics suggesting that hydrogen peroxide, if formed, did not interfere with the oxidation reaction. In contrast, the deviation was suppressed with the addition of SOD (0.2 or 0.4  $\mu\text{M}$ ), implicating superoxide radical formation. A plausible explanation for this behavior is that, in the absence of SOD, both dioxygen and superoxide radical oxidize Fe(II)CBS. Superoxide radicals can originate from the oxidation of CBS itself as well as from the autooxidation of dithionite (via reaction of its dissociation product  $\text{SO}_2^{\cdot-}$  with dioxygen). Kinetic simulations of the reactions presented in Table 1 were performed. The reaction course was well reproduced by inclusion of the reaction of superoxide radical with Fe(II)CBS with rate constants on the order of  $10^6 \text{ M}^{-1} \text{ s}^{-1}$  (Figure 3). In contrast, the reaction of hydrogen peroxide with Fe(II)CBS was characterized by a slower rate constant of  $(5.8 \pm 0.1) \times 10^3 \text{ M}^{-1} \text{ s}^{-1}$  (Supporting Information, Figure S1), and its inclusion in the simulations did not affect the aerobic decay of Fe(II)CBS.

To determine the second-order rate constant for the reaction of Fe(II)CBS with dioxygen, the pseudo-first-order rate constants for Fe(II)CBS decay were measured in the

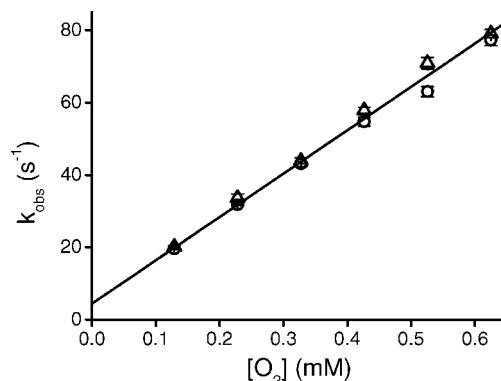


FIGURE 4: Rate constant for Fe(II)CBS reaction with  $\text{O}_2$ . An anaerobic solution of Fe(II)CBS (5  $\mu\text{M}$ ) was mixed with increasing dioxygen concentrations in sodium phosphate buffer (0.1 M, pH 7.4, with 0.1 mM DTPA) at 25 °C, in the presence of SOD (0.25  $\mu\text{M}$ ). The  $k_{\text{obs}}$  ( $\text{s}^{-1}$ ) values were determined from the fit of the exponential decay of Fe(II)CBS at 449 nm to a single exponential function at each dioxygen concentration. Results are represented as the mean  $\pm$  standard deviation ( $n \geq 8$ ). Data from two independent experiments are shown.

presence of SOD (0.25  $\mu\text{M}$ ) at increasing dioxygen concentrations. The observed rate constants increased linearly with dioxygen concentration (Figure 4), showing no evidence of saturation behavior. From the slope of the plot, the second-order rate constant was determined to be  $(1.11 \pm 0.07) \times 10^5 \text{ M}^{-1} \text{ s}^{-1}$  at pH 7.4 and 25 °C (average  $\pm$  standard deviation,  $n = 4$ ). A nonzero intercept ( $5.5 \pm 1.2 \text{ s}^{-1}$ ) was detected, and its origin is unknown. For full-length CBS, a similar reactivity as truncated CBS was observed, with a second-order rate constant of  $(1.13 \pm 0.05) \times 10^5 \text{ M}^{-1} \text{ s}^{-1}$  (Supporting Information, Figure S2).

**Superoxide Radical Generation by Fe(II)CBS Exposed to Dioxygen.** Superoxide radical can act both as a reductant and as an oxidant. We initially attempted to detect its formation by the reduction of ferricytochrome *c* or nitroblue tetrazolium (NBT) (39, 43, 44). However, when dithionite-reduced CBS was incubated with ferricytochrome *c* or NBT, the dyes were reduced even before dioxygen was added. This problem was not circumvented by gel filtration of reduced CBS under anaerobic conditions. As an alternative, epinephrine oxidation to adrenochrome, which is a useful assay for superoxide radical detection, was employed (39, 40). Exposure of Fe(II)CBS to dioxygen led to adrenochrome formation monitored by an increase in absorbance at 480 nm, which was significantly inhibited by SOD, confirming the generation of superoxide radical (Figure 5A). The UV-visible absorption spectrum showed an additional peak at  $\sim 350 \text{ nm}$  consistent with formation of an adrenochrome derivative. Adrenochrome has been reported to react with reductants such as dithionite and its decomposition product sulfite ( $\text{SO}_3^{2-}$ ) leading to an adrenochrome-sulfite complex that absorbs at 350 nm (45). We confirmed the formation of the 350 nm derivative of adrenochrome when sodium sulfite, dithionite and dithionite that had been previously decomposed in buffer were added to adrenochrome (Supporting Information, Figures S3 and S4). From these experiments, the extinction coefficient determined for the adrenochrome derivative was estimated to be  $14\,500 \pm 330 \text{ M}^{-1} \text{ cm}^{-1}$  at 350 nm.

The stoichiometry of epinephrine oxidation by superoxide radical was determined by comparing the rate of adrenochrome

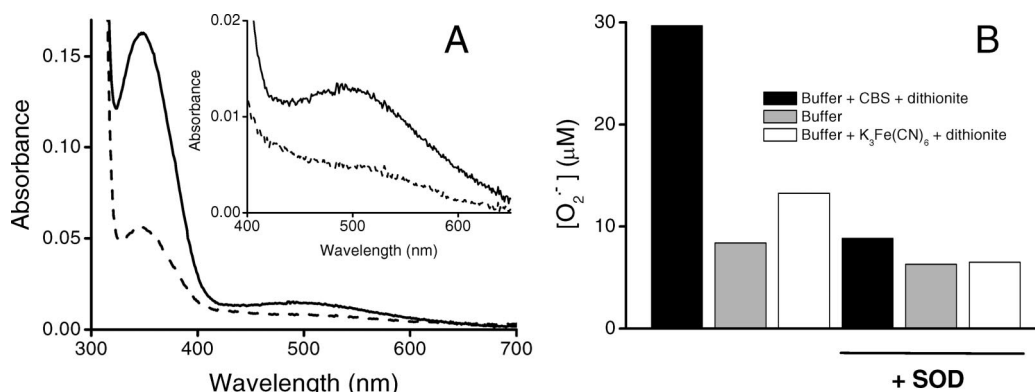


FIGURE 5: Superoxide radical detection by Fe(II)CBS reaction with dioxygen in the presence of epinephrine. (A) Anaerobic CBS (25  $\mu$ M) was reduced with dithionite (12.5  $\mu$ M) and mixed with epinephrine (2 mM) and dioxygen (200  $\mu$ M) in the absence (solid line) or in the presence of 1.5  $\mu$ M SOD (dashed line). Inset: Close-up of the 400–650 nm region. (B) Superoxide radical concentration was determined from the adrenochrome detected at 480 nm plus the adrenochrome-sulfite product at 350 nm. For controls, ferricyanide (25  $\mu$ M), which does not yield superoxide, was added. Data are representative of three independent experiments that varied by less than 10%.

chrome formation with that of ferricytochrome *c* reduction using xanthine/xanthine oxidase as a source of superoxide radical (Supporting Information, Figure S5). By comparison to the molar ratio of 1.0 for ferrocycytochrome *c* to superoxide radical, we estimated that under our experimental conditions, 1.78 mol of superoxide radical is required for the formation of 1 mol of adrenochrome at pH 8.6, which is consistent with the reported value of 1.39 at pH 7.8 (40). We also determined that, in our conditions, hydrogen peroxide (1–40 mM) did not oxidize epinephrine (data not shown).

The superoxide radical yield from CBS calculated from the products at 480 and 350 nm is shown in Figure 5B. Since adrenochrome can also be formed by epinephrine autoxidation, controls lacking CBS were included both in the absence and in the presence of dithionite. The yield of superoxide radical was consistently more than 2-fold higher in the presence of CBS. Although this assay does not provide accurate quantitative information, the results support the conclusion that superoxide radical is formed during reaction of Fe(II)CBS with dioxygen.

## DISCUSSION

In this study, we report the reduction potential of the heme in a truncated and highly active form of human CBS for which crystal structures exist (7, 8). Potentiometric titrations in the presence of mediators indicated that the heme iron in CBS undergoes reversible reduction and yielded a reduction potential of  $-291 \pm 5$  mV at pH 7.2. A relatively low redox potential for CBS was predicted based on the presence of a low spin heme with two relatively strong axial ligands. The measured value is within the range seen for other heme-thiolate proteins such as chloroperoxidase ( $-140$  mV (46)), cytochrome P450 ( $-360$  to  $-170$  mV (47)), nitric oxide synthase ( $-347$  to  $-239$  mV (48)), and *R. rubrum* CoxA ( $-320$  mV (49)). It can also be compared to other Cys/His liganded hemes such as the cytochrome *c* Met80Cys axial ligand mutant ( $-390$  mV) (50), the persulfide-modified SoxAX from *P. pantotrophus* ( $-432$  mV) (51), the cytochrome bound to the reaction center from *R. sulfidophilum* ( $-160$  mV) (12), and the His92Cys mutant of cytochrome *c*<sub>550</sub> from *T. elongatus* ( $-300$  mV) (52). In CBS, the thiolate is engaged in polar interactions with Arg266 and the main chain nitrogen of Trp54 (7, 8). These interactions, by

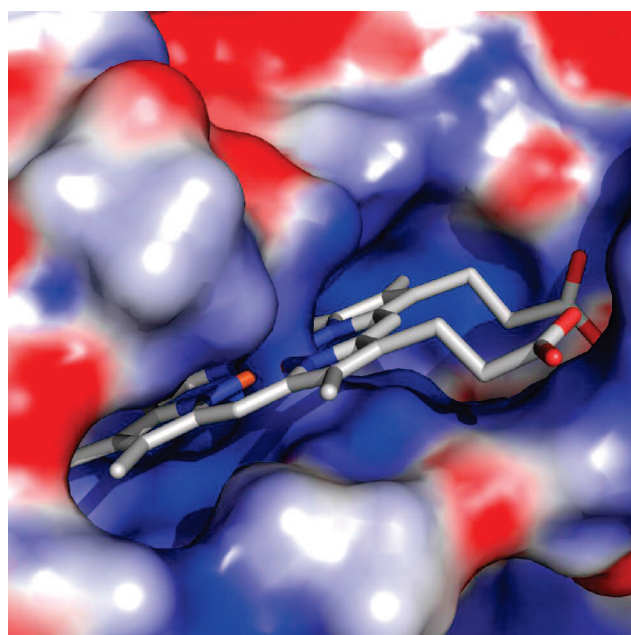


FIGURE 6: Three-dimensional structure of the heme binding site showing the electrostatic potential. The heme is shown in stick display and the protein surface is colored according to the surface potential with positive regions in blue and negative regions in red. Atomic coordinates were downloaded from the Protein Data Bank, accession code 1JBQ (7). The figure was prepared with PyMol v0.99 (68), and electrostatic calculations in vacuum were performed with the Adaptive Poisson–Boltzmann Solver (APBS) (69) using the Amber force field.

diminishing the electron donation to the metal center, would tend to stabilize the reduced state and increase the redox potential (53, 54). The heme pocket in CBS appears to be largely electropositive, with several positively charged residues within close range of the heme including Arg51 and Arg224, which interact with the heme carboxylates (Figure 6). Such an electropositive environment is predicted to have a stabilizing effect on the reduced state. In contrast to other proteins where the heme is buried in an internal cavity, the heme in CBS appears to be fairly surface exposed ( $\sim 150$  Å<sup>2</sup>). We note however that the N-terminal  $\sim 40$  amino acid residues of CBS are not seen in the crystal structure and their influence on heme exposure is not known.

Considering that the one electron reduction potential of dioxygen,  $E^\circ(\text{O}_2/\text{O}_2^{\bullet-})$ , is  $-160$  mV (1 M O<sub>2</sub> standard state)

(55), the formation of superoxide radical is favored thermodynamically. Indeed, our studies indicate that superoxide radical is formed from Fe(II)CBS oxidation (Figure 5). Superoxide radical can also oxidize Fe(II)CBS, by virtue of its relatively high reduction potential of  $E^{\circ'}(\text{O}_2^{\cdot-}, 2\text{H}^+/\text{H}_2\text{O}_2) = +940 \text{ mV}$  (56). Using kinetic simulations, we estimated a value of  $2\text{--}10 \times 10^6 \text{ M}^{-1} \text{ s}^{-1}$  for this reaction. However, this is unlikely to be significant in vivo, since the main fates of superoxide radical are dismutation to hydrogen peroxide and dioxygen catalyzed by SOD ( $2 \times 10^9 \text{ M}^{-1} \text{ s}^{-1}$ ) (57) and reaction with nitric oxide leading to peroxynitrite ( $1.9 \times 10^{10} \text{ M}^{-1} \text{ s}^{-1}$ ) (58).

The oxidation of CBS by dioxygen appears to proceed directly from the ferrous to the ferric state, presumably via an outer sphere electron transfer reaction with a second-order rate constant of  $(1.11 \pm 0.07) \times 10^5 \text{ M}^{-1} \text{ s}^{-1}$  at pH 7.4 and 25 °C. This agrees with the absence of detectable intermediates, with the linear (versus saturable) kinetics of oxidation and with the reported slow dissociation of the cysteine ligand ( $0.0166 \text{ s}^{-1}$ ) (26). Although autooxidation mechanisms proposed for most heme proteins involve dioxygen binding to the metal center (59), outer sphere processes have been proposed for some systems (60, 61). In addition, kinetic properties similar to those observed for CBS have been reported for the phagocytic cytochrome  $b_{558}$  component of NADPH oxidase, which reacts with dioxygen at  $9.3 \times 10^6 \text{ M}^{-1} \text{ s}^{-1}$  to produce superoxide radical (62).

The reduction potential estimated herein is high enough to allow CBS to be reduced in vivo. If reduced in the cell, the heme is expected to be rapidly oxidized by dioxygen. At a dioxygen concentration of  $56 \mu\text{M}$  (63, 64), we calculate a pseudo-first-order rate constant for reoxidation of  $5.8 \text{ s}^{-1}$  (half-life 0.12 s). In contrast, the dissociation of the cysteine ligand, which is rate limiting for CO binding, occurs at  $0.0166 \text{ s}^{-1}$  (26), and the thermally induced ligand switch to the CBS424 species occurs at unappreciable rates at pH 7.4 and 25 °C (23).

If CBS does indeed exist in the reduced state in vivo, it will constitute a previously unrecognized source of superoxide radical in the cytosolic compartment, and possibly, in the nucleus. Superoxide radical and its downstream products such as hydrogen peroxide and peroxynitrite are not only key contributors of oxidative stress but also trigger novel signaling mechanisms. Hence, the rapid reaction between CBS and dioxygen adds an important new element in our understanding of the possible roles of the heme in CBS.

## ACKNOWLEDGMENT

We thank Drs. Gerardo Ferrer and Matías Möller (Facultad de Ciencias, Uruguay) for helpful discussions.

## SUPPORTING INFORMATION AVAILABLE

Figures showing the reaction of truncated Fe(II)CBS with hydrogen peroxide, the reaction of full-length Fe(II)CBS with dioxygen, the effect of reductants on adrenochrome, and the stoichiometry of adrenochrome formation from superoxide radical are available free of charge via the Internet at <http://pubs.acs.org>.

## REFERENCES

- Kraus, J. P., Janosik, M., Kozich, V., Mandell, R., Shih, V., Sperandio, M. P., Sebastiao, G., de Franchis, R., Andria, G., Kluijtmans, L. A., Blom, H., Boers, G. H., Gordon, R. B., Kamoun, P., Tsai, M. Y., Kruger, W. D., Koch, H. G., Ohura, T., and Gaustadnes, M. (1999) Cystathionine beta-synthase mutations in homocystinuria. *Hum. Mutat.* 13, 362–375.
- Mills, J. L., McPartlin, J. M., Kirke, P. N., Lee, Y. J., Conley, M. R., Weir, D. G., and Scott, J. M. (1995) Homocysteine metabolism in pregnancies complicated by neural-tube defects. *Lancet* 345, 149–151.
- Refsum, H., Ueland, P. M., Nygard, O., and Vollset, S. E. (1998) Homocysteine and cardiovascular disease. *Annu. Rev. Med.* 49, 31–62.
- Kabil, O., Zhou, Y., and Banerjee, R. (2006) Human cystathionine beta-synthase is a target for sumoylation. *Biochemistry* 45, 13528–13536.
- Kery, V., Poneleit, L., and Kraus, J. P. (1998) Trypsin cleavage of human cystathionine beta-synthase into an evolutionarily conserved active core: structural and functional consequences. *Arch. Biochem. Biophys.* 355, 222–232.
- Taoka, S., Widjaja, L., and Banerjee, R. (1999) Assignment of enzymatic functions to specific regions of the PLP-dependent heme protein cystathionine beta-synthase. *Biochemistry* 38, 13155–13161.
- Meier, M., Janosik, M., Kery, V., Kraus, J. P., and Burkhard, P. (2001) Structure of human cystathionine beta-synthase: a unique pyridoxal 5'-phosphate-dependent heme protein. *EMBO J.* 20, 3910–3916.
- Taoka, S., Lepore, B. W., Kabil, O., Ojha, S., Ringe, D., and Banerjee, R. (2002) Human cystathionine beta-synthase is a heme sensor protein. Evidence that the redox sensor is heme and not the vicinal cysteines in the CXXC motif seen in the crystal structure of the truncated enzyme. *Biochemistry* 41, 10454–10461.
- Zou, C. G., and Banerjee, R. (2003) Tumor necrosis factor- $\alpha$ -induced targeted proteolysis of cystathionine beta-synthase modulates redox homeostasis. *J. Biol. Chem.* 278, 16802–16808.
- Kery, V., Bukovska, G., and Kraus, J. P. (1994) Transsulfuration depends on heme in addition to pyridoxal 5'-phosphate. Cystathionine beta-synthase is a heme protein. *J. Biol. Chem.* 269, 25283–25288.
- Cheesman, M. R., Little, P. J., and Berks, B. C. (2001) Novel heme ligation in a c-type cytochrome involved in thiosulfate oxidation: EPR and MCD of SoxAX from *Rhodovulum sulfidophilum*. *Biochemistry* 40, 10562–10569.
- Alric, J., Tsukatani, Y., Yoshida, M., Matsura, K., Shimada, K., Hienerwadel, R., Schoep-Cohenet, B., Nitschke, W., Nagashima, K. V., and Vermeglio, A. (2004) Structural and functional characterization of the unusual triheme cytochrome bound to the reaction center of *Rhodovulum sulfidophilum*. *J. Biol. Chem.* 279, 26090–26097.
- de Rosny, E., de Groot, A., Jullian-Binard, C., Gaillard, J., Borel, F., Pebay-Peyroula, E., Fontecilla-Camps, J. C., and Jouve, H. M. (2006) Drosophila nuclear receptor E75 is a thiolate hemoprotein. *Biochemistry* 45, 9727–9734.
- Igarashi, J., Sato, A., Kitagawa, T., Yoshimura, T., Yamauchi, S., Sagami, I., and Shimizu, T. (2004) Activation of heme-regulated eukaryotic initiation factor 2 $\alpha$  kinase by nitric oxide is induced by the formation of a five-coordinate NO-heme complex: optical absorption, electron spin resonance, and resonance raman spectral studies. *J. Biol. Chem.* 279, 15752–15762.
- Taoka, S., Ohja, S., Shan, X., Kruger, W. D., and Banerjee, R. (1998) Evidence for heme-mediated redox regulation of human cystathionine beta-synthase activity. *J. Biol. Chem.* 273, 25179–25184.
- Kabil, O., Taoka, S., LoBrutto, R., Shoemaker, R., and Banerjee, R. (2001) Pyridoxal phosphate binding sites are similar in human heme-dependent and yeast heme-independent cystathionine beta-synthases. Evidence from  $^{31}\text{P}$  NMR and pulsed EPR spectroscopy that heme and PLP cofactors are not proximal in the human enzyme. *J. Biol. Chem.* 276, 19350–19355.
- Jhee, K. H., McPhie, P., and Miles, E. W. (2000) Yeast cystathionine beta-synthase is a pyridoxal phosphate enzyme but, unlike the human enzyme, is not a heme protein. *J. Biol. Chem.* 275, 11541–11544.
- Janosik, M., Oliveriusova, J., Janosikova, B., Sokolova, J., Kraus, E., Kraus, J. P., and Kozich, V. (2001) Impaired heme binding and aggregation of mutant cystathionine beta-synthase subunits in homocystinuria. *Am. J. Hum. Genet.* 68, 1506–1513.

19. Ojha, S., Wu, J., LoBrutto, R., and Banerjee, R. (2002) Effects of heme ligand mutations including a pathogenic variant, H65R, on the properties of human cystathionine beta-synthase. *Biochemistry* 41, 4649–4654.
20. Katsushima, F., Oliveriusova, J., Sakamoto, O., Ohura, T., Kondo, Y., Inuma, K., Kraus, E., Stouracova, R., and Kraus, J. P. (2006) Expression study of mutant cystathionine beta-synthase found in Japanese patients with homocystinuria. *Mol. Genet. Metab.* 87, 323–328.
21. Kim, C. E., Gallagher, P. M., Guttormsen, A. B., Refsum, H., Ueland, P. M., Ose, L., Folling, I., Whitehead, A. S., Tsai, M. Y., and Kruger, W. D. (1997) Functional modeling of vitamin responsiveness in yeast: a common pyridoxine-responsive cystathionine beta-synthase mutation in homocystinuria. *Hum. Mol. Genet.* 6, 2213–2221.
22. Taoka, S., Green, E. L., Loehr, T. M., and Banerjee, R. (2001) Mercuric chloride-induced spin or ligation state changes in ferric or ferrous human cystathionine beta-synthase inhibit enzyme activity. *J. Inorg. Biochem.* 87, 253–259.
23. Pazicni, S., Cherney, M. M., Lukat-Rodgers, G. S., Oliveriusova, J., Rodgers, K. R., Kraus, J. P., and Burstyn, J. N. (2005) The heme of cystathionine beta-synthase likely undergoes a thermally induced redox-mediated ligand switch. *Biochemistry* 44, 16785–16795.
24. Taoka, S., West, M., and Banerjee, R. (1999) Characterization of the heme and pyridoxal phosphate cofactors of human cystathionine beta-synthase reveals nonequivalent active sites. *Biochemistry* 38, 2738–2744.
25. Taoka, S., and Banerjee, R. (2001) Characterization of NO binding to human cystathionine beta-synthase: possible implications of the effects of CO and NO binding to the human enzyme. *J. Inorg. Biochem.* 87, 245–251.
26. Puranik, M., Weeks, C. L., Lahaye, D., Kabil, O., Taoka, S., Nielsen, S. B., Groves, J. T., Banerjee, R., and Spiro, T. G. (2006) Dynamics of carbon monoxide binding to cystathionine beta-synthase. *J. Biol. Chem.* 281, 13433–13438.
27. Shan, X., and Kruger, W. D. (1998) Correction of disease-causing CBS mutations in yeast. *Nat. Genet.* 19, 91–93.
28. Kashiwamata, S., and Greenberg, D. M. (1970) Studies on cystathionine synthase of rat liver. Properties of the highly purified enzyme. *Biochim. Biophys. Acta* 212, 488–500.
29. Bradford, M. M. (1976) A rapid and sensitive method for the quantitation of microgram quantities of protein utilizing the principle of protein-dye binding. *Anal. Biochem.* 72, 248–254.
30. Berry, E. A., and Trumpower, B. L. (1987) Simultaneous determination of hemes a, b, and c from pyridine hemochrome spectra. *Anal. Biochem.* 161, 1–15.
31. Ellman, G., and Lysko, H. (1979) A precise method for the determination of whole blood and plasma sulfhydryl groups. *Anal. Biochem.* 93, 98–102.
32. Frank, N., Kery, V., Maclean, K. N., and Kraus, J. P. (2006) Solvent-accessible cysteines in human cystathionine beta-synthase: crucial role of cysteine 431 in S-adenosyl-L-methionine binding. *Biochemistry* 45, 11021–11029.
33. Schellenberg, K. A., and Hellerman, L. (1958) Oxidation of reduced diphosphopyridine nucleotide. *J. Biol. Chem.* 231, 547–556.
34. Balahura, R. J., and Johnson, M. D. (1987) Outer-sphere dithionite reductions of metal complexes. *Inorg. Chem.* 26, 3860–3863.
35. Dutton, P. L. (1978) Redox potentiometry: determination of midpoint potentials of oxidation-reduction components of biological electron-transfer systems. *Methods Enzymol.* 54, 411–435.
36. Fultz, M. L., and Durst, R. A. (1982) Mediator compounds for the electrochemical study of biological redox systems: a compilation. *Anal. Chim. Acta* 140, 1–18.
37. Dawson, R. M. C., Elliott D. C., Elliott, W. H., and Jones, K. M. (1986) *Data for Biochemical Research*, 3rd ed., Walton Street, Oxford, New York.
38. Mendes, P. (1997) Biochemistry by numbers: simulation of biochemical pathways with Gepasi 3. *Trends Biochem. Sci.* 22, 361–363.
39. McCord, J. M., and Fridovich, I. (1969) Superoxide dismutase. An enzymic function for erythrocuprein (hemocuprein). *J. Biol. Chem.* 244, 6049–6055.
40. Misra, H. P., and Fridovich, I. (1971) The generation of superoxide radical during the autoxidation of ferredoxins. *J. Biol. Chem.* 246, 6886–6890.
41. Green, S., Mazur, A., and Shorr, E. (1956) Mechanism of the catalytic oxidation of adrenaline by ferritin. *J. Biol. Chem.* 220, 237–255.
42. Pazicni, S., Lukat-Rodgers, G. S., Oliveriusova, J., Rees, K. A., Parks, R. B., Clark, R. W., Rodgers, K. R., Kraus, J. P., and Burstyn, J. N. (2004) The redox behavior of the heme in cystathionine beta-synthase is sensitive to pH. *Biochemistry* 43, 14684–14695.
43. Massey, V. (1959) The microestimation of succinate and the extinction coefficient of cytochrome c. *Biochim. Biophys. Acta* 34, 255–256.
44. Beauchamp, C., and Fridovich, I. (1971) Superoxide dismutase: improved assays and an assay applicable to acrylamide gels. *Anal. Biochem.* 44, 276–287.
45. Heacock, R. A. (1959) The chemistry of adrenochrome and related compounds. *Chem. Rev.* 59, 181–237.
46. Makino, R., Chiang, R., and Hager, L. P. (1976) Oxidation-reduction potential measurements on chloroperoxidase and its complexes. *Biochemistry* 15, 4748–4754.
47. Huang, Y. Y., Hara, T., Sligar, S., Coon, M. J., and Kimura, T. (1986) Thermodynamic properties of oxidation-reduction reactions of bacterial, microsomal, and mitochondrial cytochromes P-450: an entropy-enthalpy compensation effect. *Biochemistry* 25, 1390–1394.
48. Presta, A., Weber-Main, A. M., Stankovich, M. T., and Stuehr, D. J. (1998) Comparative effects of substrates and pterin cofactor on the heme midpoint potential in inducible and neuronal nitric oxide synthases. *J. Am. Chem. Soc.* 120, 9460–9465.
49. Nakajima, H., Honma, Y., Tawara, T., Kato, T., Park, S. Y., Miyatake, H., Shiro, Y., and Aono, S. (2001) Redox properties and coordination structure of the heme in the co-sensing transcriptional activator CoxA. *J. Biol. Chem.* 276, 7055–7061.
50. Raphael, A. L., and Gray, H. B. (1991) Semisynthesis of axial-ligand (position 80) mutants of cytochrome c. *J. Am. Chem. Soc.* 113, 1038–1040.
51. Reijerse, E. J., Sommerhalter, M., Hellwig, P., Quentmeier, A., Rother, D., Laurich, C., Bothe, E., Lubitz, W., and Friedrich, C. G. (2007) The unusual redox centers of SoxXA, a novel c-type heme-enzyme essential for chemotrophic sulfur-oxidation of *Paracoccus pantotrophus*. *Biochemistry* 46, 7804–7810.
52. Kirilovsky, D., Roncel, M., Boussac, A., Wilson, A., Zurita, J. L., Ducruet, J. M., Bottin, H., Sugiura, M., Ortega, J. M., and Rutherford, A. W. (2004) Cytochrome c550 in the cyanobacterium *Thermosynechococcus elongatus*: study of redox mutants. *J. Biol. Chem.* 279, 52869–52880.
53. Dawson, J. H. (1988) Probing structure-function relations in heme-containing oxygenases and peroxidases. *Science* 240, 433–439.
54. Poulos, T. L. (1996) The role of the proximal ligand in heme enzymes. *J. Biol. Inorg. Chem.* 1, 356–359.
55. Wood, P. (1987) The two redox potentials for oxygen reduction to superoxide. *Trends Biochem. Sci.* 12, 250–251.
56. Koppenol, W. H. (1985) The reaction of ferrous EDTA with hydrogen peroxide: evidence against hydroxyl radical formation. *J. Free Radical Biol. Med.* 1, 281–285.
57. Klug, D., Rabani, J., and Fridovich, I. (1972) A direct demonstration of the catalytic action of superoxide dismutase through the use of pulse radiolysis. *J. Biol. Chem.* 247, 4839–4842.
58. Kissner, R., Nauser, T., Bugnon, P., Lye, P. G., and Koppenol, W. H. (1997) Formation and properties of peroxynitrite as studied by laser flash photolysis, high-pressure stopped-flow technique, and pulse radiolysis. *Chem. Res. Toxicol.* 10, 1285–1292.
59. Gonzalez, G., Gilles-Gonzalez, M. A., Rybak-Akimova, E. V., Buchalova, M., and Busch, D. H. (1998) Mechanisms of autoxidation of the oxygen sensor FixL and Aplysia myoglobin: implications for oxygen-binding heme proteins. *Biochemistry* 37, 10188–10194.
60. Chu, M. M., Castro, C. E., and Hathaway, G. M. (1978) Oxidation of low-spin iron(II) porphyrins by molecular oxygen. An outer sphere mechanism. *Biochemistry* 17, 481–486.
61. Butler, J., Koppenol, W. H., and Margoliash, E. (1982) Kinetics and mechanism of the reduction of ferricytochrome c by the superoxide anion. *J. Biol. Chem.* 257, 10747–10750.
62. Isogai, Y., Iizuka, T., Makino, R., Iyanagi, T., and Oori, Y. (1993) Superoxide-producing cytochrome b. Enzymatic and electron paramagnetic resonance properties of cytochrome b558 purified from neutrophils. *J. Biol. Chem.* 268, 4025–4031.
63. Torres Filho, I. P., Leunig, M., Yuan, F., Intaglietta, M., and Jain, R. K. (1994) Noninvasive measurement of microvascular and interstitial oxygen profiles in a human tumor in SCID mice. *Proc. Natl. Acad. Sci. U. S. A.* 91, 2081–2085.

64. Lancaster, J. R., Jr. (2006) Nitroxidative, nitrosative, and nitrative stress: kinetic predictions of reactive nitrogen species chemistry under biological conditions. *Chem. Res. Toxicol.* 19, 1160–1174.
65. Lambeth, D. O., and Palmer, G. (1973) The kinetics and mechanism of reduction of electron transfer proteins and other compounds of biological interest by dithionite. *J. Biol. Chem.* 248, 6095–6103.
66. Creutz, C., and Sutin, N. (1974) Kinetics of the reactions of sodium dithionite with dioxygen and hydrogen peroxide. *Inorg. Chem.* 13, 2041–2043.
67. Fridovich, I. (1989) Superoxide dismutases. An adaptation to a paramagnetic gas. *J. Biol. Chem.* 264, 7761–7764.
68. DeLano, W. L. (2002) in DeLano Scientific, San Carlos, CA, USA. <http://www.pymol.org>.
69. Baker, N. A., Sept, D., Joseph, S., Holst, M. J., and McCammon, J. A. (2001) Electrostatics of nanosystems: application to microtubules and the ribosome. *Proc. Natl. Acad. Sci. U. S. A.* 98, 10037–10041.

BI700912K